Molecular Genetics and Metabolism Reports 36 (2023) 100990

Contents lists available at ScienceDirect

Molecular Genetics and Metabolism Reports

journal homepage: www.elsevier.com/locate/ymgmr

Clinical, genetic, and structural characterization of a novel TUBB4B tubulinopathy

Jason R. McFadden [a,1], Christina Deanne P. Tolete [a,1], Yan Huang [a], Ellen Macnamara [a], David Sept [b], Galina Nesterova [a], William A. Gahl [a,c], Dan L. Sackett [d], May Christine V. Malicdan [a,c,*]

[a] NIH Undiagnosed Diseases Program, National Human Genome Research Institute, NIH, Bethesda, MD 20892, USA
[b] Departments of Biomedical Engineering and Biophysics, University of Michigan, Ann Arbor, MI 48109, USA
[c] Medical Genetics Branch, National Human Genome Research Institute, NIH, Bethesda, MD 20892-1851, USA
[d] Eunice Kennedy Shriver National Institute of Child Health and Human Development, NIH, Bethesda, MD 20892, USA

ARTICLE INFO

Keywords:
Microtubules
Rare disease
Tubulinopathies
Fanconi syndrome
Translational medicine

ABSTRACT

Microtubules are cytoskeletal polymers of α/β-tubulin heterodimers essential for a wide range of cellular processes. Pathogenic variations in microtubule-encoding genes (e.g., *TUBB4B*, which encodes the β-4B tubulin isotype) are responsible for a wide spectrum of cerebral malformations, collectively referred to as "tubulinopathies." The phenotypic manifestation of *TUBB4B*-associated tubulinopathy is Leber congenital amaurosis with early-onset deafness (LCAEOD), an autosomal dominant syndrome characterized by photoreceptor and cochlear cell loss; all known patients have pathogenic variations in amino acid R391. We present the clinical and molecular genetics findings of a 16-year-old female with a de novo missense variant in exon 1 of *TUBB4B*, c.32 A > G (p.Gln11Arg; Q11R). In addition to hearing loss and hyperopia without retinal abnormalities, our proband presented with two phenotypes of unknown genetic etiology, i.e., renal tubular Fanconi Syndrome (FS) and hypophosphatemic rickets (HR). The Q11R variant expands the genetic basis of early sensory hearing loss; its consequences with respect to microtubule structure are described. A mechanistic explanation for the FS and rickets, involving microtubule-mediated translocation of transporter proteins to and from the apical membrane of renal proximal tubular cells, is proposed.

1. Introduction

Microtubules are cytoskeletal polymers of α/β-tubulin heterodimers with numerous cellular functions, including intracellular transport, axonal guidance, ciliary and flagellar motility, and mitotic spindle assembly [1,2]. The functional diversity of microtubules is attributed to their post-translational modifications and tissue-specific expressions [3]. Dynamic instability (i.e., the ability to stochastically polymerize and depolymerize) is an essential feature of microtubules, as it allows for their structural reorganization in response to cellular needs. For example, during metaphase, kinetochore-associated microtubules polymerize at their plus-ends (closest to the kinetochore) and depolymerize at their minus-ends (closest to the centrosome), allowing for alignment of chromosomes along the metaphase plate [4]. During anaphase, the plus-ends depolymerize, resulting in the movement of chromatids to opposite poles of the cell. The dynamic instability of microtubules is modulated by both stabilizing proteins (e.g., XMAP215, MAP65/Ase1/PRC1, +TIPS, MAP61, the γ-tubulin ring complex) and destabilizing proteins (e.g., Kinesin-8, Kinesin-13) [4]. Disruption of dynamic instability, or of the proteins involved in regulating dynamic instability, has been implicated in numerous pathologies [5,6].

All α- and β-tubulin isotypes are encoded by the *TUB* gene family (Table 1). Pathogenic variations in *TUB* family genes can alter microtubule stability and lead to "tubulinopathies" with heterogeneous clinical manifestations. The *TUBB4B* gene (formerly *TUBB2* or *TUBB2C*) encodes the β-4B tubulin isotype and is ubiquitously expressed in embryonic and adult tissues, especially the retina, testis, and bone marrow [National Library of Medicine, 2022]. Monoallelic variants in amino acid R391 of the TUBB4B protein have been associated with Leber Congenital Amaurosis with Early Onset Deafness (LCAEOD), an

* Corresponding author.
E-mail address: maychristine.malicdan@nih.gov (M.C.V. Malicdan).
[1] These authors contributed equally.

https://doi.org/10.1016/j.ymgmr.2023.100990
Received 24 June 2023; Accepted 25 June 2023

Table 1
Known phenotypic manifestations of tubulinopathies.

Gene	Location	Tubulin isotype*	Mutant phenotypes
TUBA1A	12q13.12	α-1a	Brain malformations, microcephaly, developmental delay, epilepsy
TUBA1B	12q13.12	α-1b	No known human disease
TUBA1C	12q13.12	α-1c	No known human disease
TUBA3C	13q12.11	α-3c	No known human disease. Reduced expression associated with poor sperm motility
TUBA3D	2q21.1	α-3d	Keratoconus: corneal ectasia, thinning, and cone-shaped protrusion that results in reduced vision
TUBA3E	2q21.1	α-3e	No known human disease
TUBA4A	2q35	α-4a	Amyotrophic lateral sclerosis, with or without frontotemporal dementia
TUBA4B	2q35	α-4b	No known human disease
TUBA8	22q11.21	α-8	Macrothrombocytopenia
TUBB	6p21.33	β	Cortical dysplasia with brain malformation and microcephaly. Congenital symmetric circumferential skin creases. Mutations are a strong predictor of response to chemotherapy (paclitaxel)
TUBB1	20q13.32	β-1	Macrothrombocytopenia
TUBB2A	6p25.2	β-2a	Complex cortical dysplasia with other brain malformations, severe global developmental delay, epilepsy
TUBB2B	6p25.2	β-2b	Complex cortical dysplasia with other brain malformations, severe global developmental delay, epilepsy
TUBB3	16q24.3	β-3	Cortical dysplasia, congenital fibrosis of extraocular muscles, basal ganglia dysmorphism, brain stem & cerebellar vermian hypoplasia
TUBB4A	19p13.3	β-4a	Torsion dystonia, dysphonia. Hypomyelinating leukodystrophy, microcephaly, hearing loss, delayed motor development, seizures
TUBB4B	9q34.3	β-4b	Leber congenital amaurosis with early-onset deafness
TUBB6	18p11.21	β-6	Congenital facial palsy with ptosis and velopharyngeal dysfunction, dysphagia
TUBB8	10p15.3	β-8	Female infertility, oocyte maturation arrest
TUBB8B	18p11.32	β-8b	No known human disease

* Isotypes refer to isotypes: α, or alpha-tubulinopathies; and β, or beta-tubulinopathies.

autosomal dominant syndrome characterized by progressive loss of photoreceptors and cochlear cells (4).

Here we present a 16-year-old female with a novel heterozygous missense variant (c.32A > G, p.Q11R) in exon 1 of *TUBB4B*. In addition to having early-onset hearing loss and hyperopia, our patient exhibited hypophosphatemic rickets (HR), renal tubular Fanconi syndrome (FS), and nephrocalcinosis. We describe the clinical characteristics of this individual and elucidate the relationship between the 3-dimensional structure of the mutant tubulin and its function. We also speculate on the mechanism by which this *TUBB4B* p.Q11R variant could be causing the patient's rickets and renal Fanconi syndrome.

2. Materials and methods

The patient was admitted to the National Institutes of Health Clinical Center (NIH-CC) as part of the NIH Undiagnosed Diseases Program [7–9]. She was enrolled in protocol 76-HG-0238, "Diagnosis and Treatment of Patients with Inborn Errors of Metabolism or Other Genetic Disorders," approved by the National Human Genome Research Institute (NHGRI) Institutional Review Board (IRB). With written informed consent from her parents, the patient underwent a 5-day clinical evaluation.

2.1. Molecular data and analysis

High-density single-nucleotide polymorphism (SNP) arrays and exome sequencing were performed on genomic DNA from the proband and her parents as described [10–12]. Exome sequencing was carried out with the TruSeq capture kit and was run on the Illumina HiSeq2000 (Illumina, San Diego, CA); short reads were aligned to the Hg19 Human reference with NovoAlign by the NHGRI Intramural Sequencing Center. Variants were prioritized based on predicted pathogenicity scores (CADD, Mutation Taster, SIFT), and population frequency (ExAc and gnomAD). Final candidate variants were validated by Sanger sequencing.

2.2. Tubulin acetylation western blot

Fibroblasts from the patient and from an age- and sex- matched healthy control were grown at 37 °C, 5% CO_2 in DMEM growth media supplemented with 10% FBS. Cells were harvested by trypsinization, washed with PBS, and lysed in SDS gel loading buffer followed by incubation at 90 °C for 3 min. Protein concentration was determined with Pierce BCA assay and equal quantities of protein were loaded on gels in duplicate. Following electrophoresis and transfer to nitrocellulose membranes, the membranes were blocked with 5% nonfat dry milk in TBS and cut in half, between the duplicate loadings. One membrane half was incubated overnight with DM1A anti-pan-alpha tubulin antibody (Sigma T6199), diluted 1:1000 in blocking buffer. The other half was incubated overnight with anti-acetylated tubulin antibody (Sigma 6-11B-1), also diluted 1:1000 in blocking buffer. Following washing with TBS and TBS + 0.05% Tween, the two membrane pieces were incubated with LiCor IR-labeled anti-mouse secondary antibody and observed with a LiCor Odyssey according to company specifications.

3. Results

3.1. Clinical findings

The patient was born by C-section at 2.72 kg, 48.3 cm to a 35 y/o G1P0 mother at 37 weeks. The pregnancy was complicated by a #100 weight gain with no hypertension. Her mother ceased smoking at six weeks' gestation; she had exposure to industrial chemicals up to the fifth month of pregnancy. The newborn had an Apgar score of 6 and failed a newborn hearing screening. Twelve hours after her birth, she was admitted to the Special Care Nursery due to grunting and lack of interest in eating, resulting in weight loss. The cause was determined to be acid reflux and mild aspiration. She was discharged after 10 days in good condition.

At 5 months, she developed pneumonia and was treated successfully at home. At 6 months, she was diagnosed with benign central hypotonia and moderate bilateral neurosensorial hearing loss. She had recurrent episodes of otitis media and underwent a tympanostomy at 8 months. Auditory Brainstem Response (ABR) testing indicated behavioral responses consistent with high-frequency hearing loss. While she was able to speak words at 10 months with hearing aids, ~70% of her sentences were incomprehensible. Further evaluation assessed sensory processing difficulties and delayed motor skills. She also had a weak jaw, which was attributed to inexperience and/or hypersensitive gag reflex. X-ray showed evidence of four healed rib fractures, a rachitic rosary, and generalized bone demineralization, with a Z score of −2.5 on DEXA scan. Serum alkaline phosphatase level was 1396 U/L (normal, 120–230 U/L).

At 10 months, an endocrinologist diagnosed renal Fanconi Syndrome, hypophosphatemic rickets, failure to thrive, hypocalcemia, hypophosphatemia, glucosuria, renal tubular acidosis, and aminoaciduria (7- to 16-fold normal levels) initially thought to be secondary to nephropathic cystinosis. Cystinosis was ruled out due to a normal leucocyte cystine level and no evidence of corneal crystals. Calcitriol, K-

citrate, and K-Phos-Neutral were added to her medication regimen. Examination at 1 year of age revealed that the proband could stand without support. She had a relatively strong trunk but exhibited weakness in all four extremities. She had neutral lower extremity alignment, although she exhibited unassisted ambulation in an externally rotated position.

At 14 months, she underwent an open renal biopsy due to fluctuating creatinine levels. G-tube placement was also performed during this surgery. Five days following the surgery, she bled from the biopsy, resulting in a significant blood clot in her bladder. A transfusion and emergency cystoscopy were performed to remove the clot, and she left the hospital and weighed 6.35 kg several weeks later.

At 15 months, she was diagnosed with hyperopia and anisometropia, prompting the use of corrective lenses. At 17 months, she underwent an adenoidectomy and PE tube replacement. At 18 months, the development of a unilateral breast bud led to an MRI and ultrasound, whose results were consistent with benign thelarche. The patient also complained of chronic nausea and vomiting, which was originally attributed to her elevated FSH levels. However, the patient was hospitalized for hypokalemia (2.1 mmol/L) two months later, and testing revealed that she has a J-shaped stomach, which was determined to be the cause of her nausea. Adjusting her feeds to lower volumes and switching to a Soy formula reduced vomiting by over half. At 22 months, chronic sinusitis was treated with antibiotics, and she had difficulty swallowing and nasal breathing.

At 35 months, the patient was admitted to the NIH Clinical Center. Upon examination, she had mild dolichocephaly, oval shape eyes, blue irises, inner canthal space of 2 cm (<2 SD below 3rd percentile), outer canthal of −5 cm (<2.5 SD), hypotelorism, upturned nose, high arched palate, normal teeth, philtrum, ear lobes, and short neck with low posterior hair line (Fig. 1A). The patient's height was 77.7 cm (−3.46 SD) (Fig. 1B) and she weighed 10.3 kg (−1.56 SD) (Fig. 1C), with a head circumference of 48 cm (32nd percentile). Her muscle tone was 2/5 in proximal muscles and 3/6 in distal muscles. Cranial nerves 2–12 were grossly intact, with unsteady DTRs of +2 in upper and lower extremities. MRI revealed an abnormally small pituitary gland, pointing to a risk for severe panhypopituitarism. Audiology consult confirmed bilateral hearing loss. Response to speech stimuli, as determined via visual reinforcement audiometry, was obtained at 50 dB HL. Her tympanometry revealed flat tympanograms with a large physical middle ear volume in the right ear (suggesting a patent PE tube) and a near-normal physical volume in the left ear (suggesting a possible non-patent PE tube). Ophthalmology consult revealed hyperopia, microcornea, and probable microphthalmia on both eyes. The patient was negative for cataract. Her corneal horizontal diameter was abnormally low (10 mm in each eye). No peripheral pigmentary changes were found upon fundus examination. Because of the history of several pneumonias and multiple upper respiratory infections and sinusitis, ciliary dyskinesia was suspected. A pulmonary consult was sought, where a recommendation for a biopsy was given but not performed. Bone series revealed low normal bone age, and a slightly enlarged craniofacial ratio with noted osteopenia. Skeletal survey revealed impaired mineralization and bowing of tibia and fibula (Fig. 1D) and DX Bone series revealed low normal bone age. Abdominal ultrasound showed a slightly enlarged liver with severe medullar nephrocalcinosis (Fig. 1E).

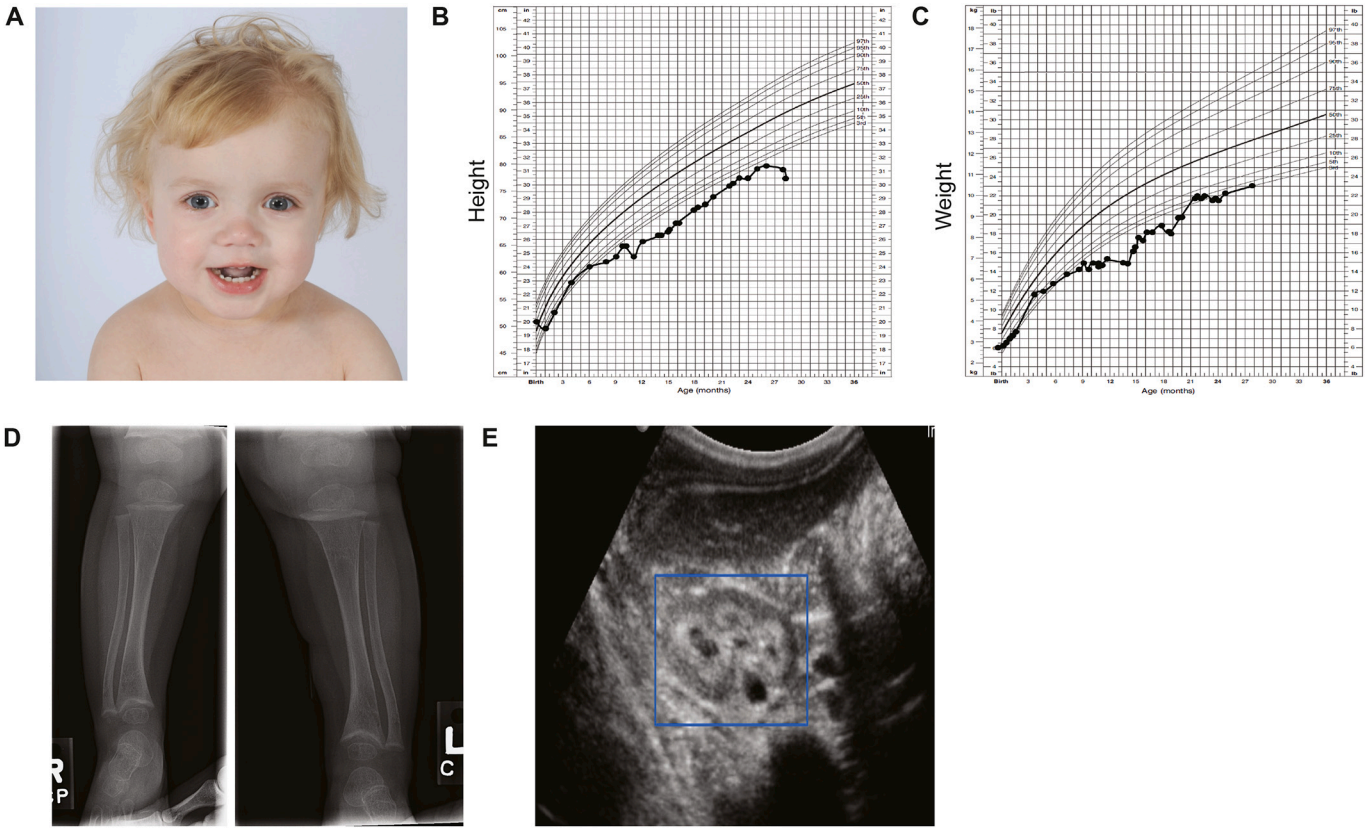

Fig. 1. Clinical features of proband. (**A**) A photograph of the proband at 35 months, showing oval shape eyes, blue irises, inner canthal space of 2 cm, outer canthal of −5 cm, hypotelorism, upturned nose, and short neck. (**B**) Growth chart showing the proband's height from birth to 36 months. On average, proband's height is below the 3rd percentile. (**C**) Growth chart showing proband's weight from birth to 36 months, generally demonstrating that the weight is below the 3rd percentile. (**D**) Representative skeletal x-ray showing reduced mineralization of the tibia and bowing of tibia and fibula. (**E**) Representative image of abdominal ultrasound demonstrating a finding of severe medullar nephrocalcinosis.

3.2. Molecular analyses

A clinical chromosomal microarray analysis and research genome-wide microarray analysis identified a copy number gain in Xp22.31 that was inherited from the proband's unaffected mother. X inactivation studies on proband's blood and fibroblasts revealed abnormal, mildly skewed X inactivation (78%:22% and 74%:26%, respectively). The mother's X inactivation study was consistent with normal, random X inactivation (53%:47%). Gene panel sequencing for Fragile X, methylation studies for Angleman syndrome, and mitochondrial sequencing were negative. Trio exome analyses revealed a de novo variant in *TUBB4B* (NM_006088.6:c.32C > G, p.Gln11Arg or p.Q11R; NC_000009.11[GRCh37]:g.140135844A > G), which was confirmed by Sanger sequencing (Fig. 2A and B). The p.Q11R variant is absent in gnomAD and 1000 genomes, has a high CADD_phred score of 24.9, is possibly damaging by Polyphen, and is in the Tubulin/FtsZ, GTPase domain of TUBB4B (Fig. 2C). By ACMG criteria it is considered likely pathogenic (PM1, located in a well-established functional domain; PM2, absent from controls; PP2, missense variant in a gene with low rate of missense variation; and PP3, computational evidence supporting deleterious effect on gene). Analyses for coding variants in genes associated with renal Fanconi syndrome (*GATM*, MIM 602360; *SLC34A1*, MIM 182309; *NDUFAF6*, MIM 612392; *EHHADH*, MIM 607037) and hypophosphatemic rickets (*FGF23*, MIM 605380; *SLC34A3*, MIM 609826; *DMP1*, MIM 600980; *ENPP1*, MIM 173335) did not reveal putative pathogenic variants.

3.3. Structural modeling

Molecular modeling of the tubulin dimer in the microtubule wall (Fig. 2D) shows that the beta Q11 residue is located at the growing (+)-end of microtubule in the inter-dimer contact, close to the bound nucleotide (GTP in the free dimer and at the microtubule end, hydrolyzed to GDP after a new dimer adds to the end, covering the exposed beta-GTP with the new alpha subunit). The sites of the Q11R varaint described here, and the R391H/C variants previously reported in [3,5] are shown on the tubulin molecules oriented as in the microtubule, viewed from the outside, and named as the WT residues. Q11 and GDP are centrally located in the interdimer contact surface, while R391 is near the back, laterally (Fig. 2D). In Fig. 2E, the protofilaments have been tilted so that the view is down the long axis of the microtubule. It is clear that Q11 is immediately adjacent to the GDP, while R391 is considerably removed from the GDP. Fig. 2F is again viewed from the outside of the microtubule, as in 2D. The central region of the αβ contact site in 2D is expanded, showing the Q11 residue (red) immediately adjacent to the GDP and its associated Mg2+, and very close to the αE254 residue (indigo). The αE254 is part of the α of the incoming αβ dimer, which is adding to the growing end of the microtubule. This E residue is essential for GTP hydrolysis, which is required for microtubule disassembly. This disassembly is critical for the dynamics of the microtubule. In this catalytic center for GTPase activity, adjacent to the anionic phosphates of the nucleotide and the anionic side group of the incoming glutamic acid residue, the Q11R variant will place the cationic (positively charged) guanidino group of the arginine.

3.4. Q11R variant effect on tubulin acetylation

The positioning of the fixed positive charge of arginine in Q11R in between / adjacent to the negative charge of the nucleotide phosphate chain (and its associated Mg2+) and the negative charge of the side chain of αE254 suggests that this will inhibit the GTPase activity that requires the αE254 side chain as half of the catalytic site. GTP hydrolysis is required for microtubule depolymerization, an essential half of the polymer dynamics of the microtubules. Inhibition of GTP hydrolysis will impede depolymerization and hence stabilize the polymerized microtubule. Since acetylation of alpha tubulin (on αLys40) often is increased on stabilized microtubules, we hypothesized that tubulin acetylation would be increased in proband fibroblasts due to the Q11R variant. Accordingly, we compared acetylated alpha tubulin staining with total alpha tubulin staining (as a normalization control) on a Western blot of proband fibroblasts compared to those from a normal control; Western blotting for acetylated tubulin is a well-established proxy for tubulin acetylation [13]. The Western blot was cut in half, and half of the blot was probed with a pan-α tubulin antibody (Fig. 2G), and the other half was probed with an antibody for acetylated alpha tubulin (Ac-αLys40) (Fig. 2H). As is clear in Fig. 2H, acetylation is enhanced in the sample of proband fibroblasts, consistent with our prediction.

4. Discussion

Luscan et al. [5] first linked heterozygous *TUBB4B* pathogenic variations to early onset hearing loss, identifying six patients with the c.1172G > A;p.Arg391His variant (four heterozygotes and two mosaics) and one patient with a c.1171C > T;p.Arg391Cys variant (Table 2). These Arg391 substitutions in the H11 helix of β-4B tubulin were shown to disrupt a key hydrophobic interaction between the longitudinally adjacent T7 loop and H8 helix of α-tubulin, thereby altering microtubule stability. Maasz et al. [3] (Table 2) reported similar clinical manifestations of three members of a Hungarian family heterozygous for the *TUBB4B* c.1171C > T (p.Arg391Cys) variant. In addition to early-onset sensorineural hearing loss, all three patients had severe ophthalmologic impairment, including anopia, retinal degeneration, strabismus, and hypermetropia. Our proband described here had early sensorineural hearing loss, hyperopia, and microcornea but no signs pointing to Leber congenital amaurosis because of the lack of nystagmus or photophobia. Nonetheless, it is of note here that all patients thus far reported have hyperopia. The ophthalmic lens is one of the tissues that rely on coordination of cytoskeletal elements, including microtubules, for optimal lens fiber cell migration and elongation for proper tissue architecture [14]. It will be interesting to identify the role of TUBB4B in lens fiber cell growth and development [14].

In addition to having auditory and ophthalmic involvement, our patient manifested renal Fanconi syndrome (aminoaciduria, glucosuria, proteinuria), nephrocalcinosis, and rickets. We could not identify a variant in a gene known to cause these disorders. Rather, we propose that the p.Q11R missense variant in *TUBB4B* and its specific location were responsible not only for the patient's auditory and ophthalmologic impairments but for her renal issues. First, p.Q11R occurs early in the sequence of β-4b tubulin and likely affects the catalytic site of GTPase activity by introducing a positive guanidino group that counteracts both the negative α-glutamate (αE245) and the negative phosphate group on the adjacent GDP; the former is required for microtubule depolymerization. In contrast, the amino acid substitutions in previously reported *TUBB4B*-associated tubulinopathy patients (R391C and R391H) do not affect this catalytic site (Fig. 2F).

Second, the p.Q11R variant could confer excess stability on our patient's microtubules; many biological processes rely on microtubule stability (inhibited depolymerization) or instability (inhibited polymerization). Evidence that p.Q11R stabilizes microtubules was found in the patient's fibroblasts, which exhibited tubulin acetylation (Fig. 2G), a well-characterized posttranslational modification that occurs in microtubules that fail to depolymerize.

Third, microtubules are known to influence renal phosphate homeostasis by their effects on solute carriers [15]. Specifically, microtubules are involved in both the upregulation (via translocation to the apical membrane) and the downregulation (via endocytosis and lysosomal degradation) of NaPi-IIa (SLCA1) and NaPi-Iic (SLCA3), two members of the SLC34 solute carrier family that govern renal phosphate homeostasis. Microtubules that are "overly stable" by virtue of the p.Q11R variant may lack regulatory control over transporter localization, preventing phosphate carriers from reaching the apical membrane of proximal tubular cells. This concept is consistent with a previous report

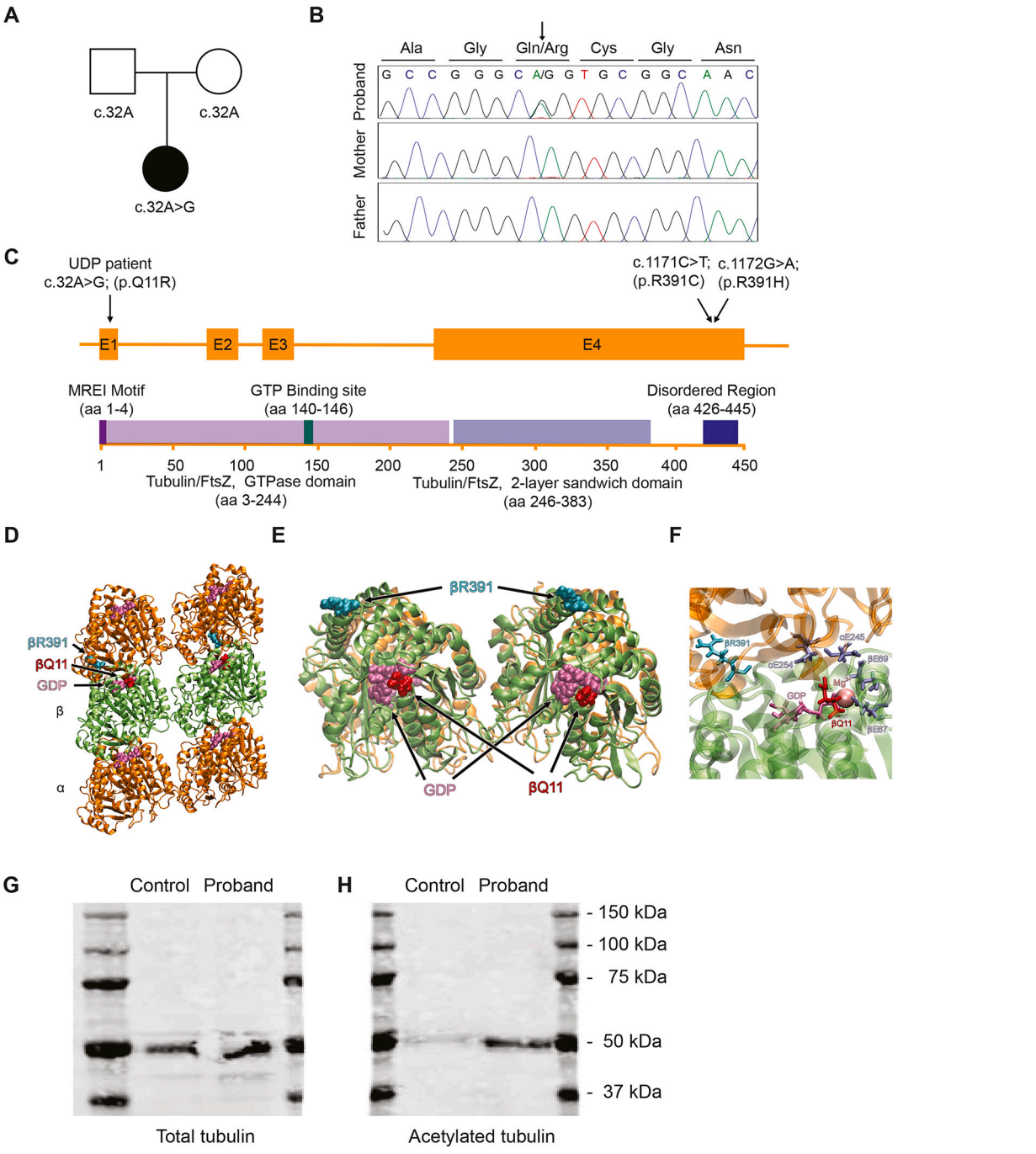

Fig. 2. Molecular and biochemical analysis. (**A**) Pedigree of the family. The proband has a variant in *TUBB4B* (c.32A > G), which is not identified in her parents, indicating a de novo pathogenic variant *TUBB4B*. (**B**) Sanger sequencing analysis chromatogram confirming the presence of a de novo variant *TUBB4B* in the proband. (**C**) Schematic representation of the *TUBB4B* gene and protein, identifying known protein domains, MREI (Met-Arg-Glu-Ile) motif, a GTP binding site, and a disordered region. (**D**) In this and in Fig. 2E and F, residue positions are indicated and named as in the WT microtubule. In 2D the microtubule is viewed from the outside. Two protofilaments have been removed from the microtubule wall and the positions of Q11 (red), R391 (cyan) and GDP (purple) are indicated. Alphas are brown and betas are green. The pair labeled α and β are the terminal αβ dimer at the growing end of the microtubule. The brown α above it is from the dimer adding to the end. (**E**) The upper alpha has been removed and the αβ dimer (labeled α and β in 2D) has been tilted so the upper surface of β in 2D is now toward the viewer. Residue Q11 can be clearly seen to be adjacent to the GDP. (**F**) The central region of the αβ contact site in D is expanded and viewed from the outside as in 2D. showing the Q11 residue (red) immediately adjacent to the GDP and its associated Mg2+, and very close to the αE254 residue (indigo), in the α of the incoming αβ dimer, which is essential for GTP hydrolysis. Western blot mages showing total (probed with a pan-alpha tubulin antibody) (**G**) and acetylated (probed with an antibody specific for acetylated alpha tubulin, acetylated at αLys40) (**H**) tubulin levels. Total tubulin levels in the proband and control appears equivalent, while tubulin acetylation is increased in the proband compared to the control.

Table 2
Clinical and molecular characteristics of patients with *TUBB4B* variants.

	This paper	II/1[a]	III/2[a]	III/1[a]	F1:II2[b]	F1:III2[b]	F1:IV1[b]	F2:I2[b]	F2:II1[b]	F3:II2[b]	F4:II3[b]
Ethnicity	Denmark/Norwegian/ German	Hungary	Hungary	Hungary	France	France	France	Algeria	Algeria	France	Denmark
TUBB4B missense variant*	c.32A > G	c.1171C > T	c.1171C > T	c.1171C > T	c.1172G > A	c.1172G > A	c.1172G > A	c.1772G > A	c.1172G > A	c.1172G > A	c.1171C > T
TUBB4B amino acid change	p.Gln11Arg	p.Arg391 Cys	p.Arg391Cys	p.Arg391 Cys	p.Arg391His	p.Arg391His	p.Arg391 His	p.Arg391 His	p.Arg391His	p.Arg391 His	p. Arg391Cys
Age at diagnosis of auditory dysfunction	Birth	3.5	NR	NR	30	7	Birth	NR	8	3	Birth
Hearing loss (Audiogram results L/R)	+	+ (80/60)	NR	NR	+ (75/70)	+ (70/70)	+ (45/45)	NR	+ (60/55)	20	+ (50/50)
Auditory brainstem response	High frequency hearing loss	NR	NR	NR	NR	100/65	NR	NR	70/60	NR	60/45
Age of ocular problem onset	NR	3	2 ¾	7 mo	30	NR	NR	NR	NR	NR	NR
Lens abnormalities	Hyperopia, with corrective lenses at 17 mo	Bilateral cataract	Astigmatism, Hypermetropia	NR	NR	Hypermetropia	Hypermetropia	NR	Hyperme-tropia, hemeralopia	NR	Hemeralo-pia
Other ocular abnormalities	Microophthalmia, microcornea, no peripheral pigmentary changes	Anopia, retinitis pigmentosa, macular pigmentary deposits	Blurred optic disc, nystagmus, retinitis pigmentosa, macular pigmentary deposits	Nystagmus, macular pigmentary deposits	Amblyopia, macular alterations, retinitis pigmentosa	Complete blindness, Photophobia, retinitis pigmentosa	Rod-cone dystrophy	NR	Photophobia, retinitis pigmentosa	Rod-cone dystrophy	Rod-cone dystrophy,
Musculoskeletal abnormalities	Osteopenia, hypophosphatemic rickets	NR	NR	NR	NR	NR	NR	NR	NR	NR	NR
Others	Hypotonia and motor development delay, hypotelorism, FTT, nephrocalcinosis	NR	NR	NR	NR		NR	NR			NR

Note: "+" = present; "NR" = not recorded; "mo" = months; FTT, failure to thrive; L, left ear, R, right ear. [a] *Maasz* et al *2022;* [b] *Luscan* et al *2017*. Accession numbers used: NM_006088.6; NP_006079.1.

[16] that showed that increased αK40 tubulin acetylation inhibits translocation of GLUT4 receptors to the plasma membrane of cardiomyocytes. Regardless of whether the mechanism is through inhibition of GLUT4 exocytosis or stimulation of GLUT4 endocytosis, a similar phenomenon may occur with respect to phosphate transporters in renal proximal tubular cells. Specifically, the p.Q11R TUBB4B variant in our proband may lead to "inadequate" translocation of SLCA1/SLCA3 to the apical membrane of proximal tubular cells, depleting serum Pi levels and contributing to the development of hypophosphatemic rickets. Since no previous cases of *TUBB4B*-tubulinopathy have exhibited renal Fanconi syndrome or hypophosphatemic rickets, this putative effect could be unique to the Q11 to arginine variant in β-4b tubulin. Transporters for other metabolites in the SLC family (e.g., SLC22A8, renal organic anion transporter 3) also rely on microtubular stability, though the exact role of microtubules differs slightly. Microtubules serve as the "tracks" on which motile Caveolin 1 (Cav1) vesicles transport SLC22A8 proteins between the basolateral membrane and specific endosomal compartments of proximal tubular cells [17]. Alteration of microtubular stability has been shown to abolish membrane localization of SLC22A8 [17].

Finally, there are several limitations to our study. First, as we did not perform whole genome sequencing, it is possible that other putative genes—or intronic variants—may partially account for our patient's symptoms. Second, we did not perform experiments to verify whether our patient's microtubular network is indeed malformed. Thus, even if this TUBB4B variant is the causative agent of our patient's symptoms, future experiments are needed to confirm this mechanistic hypothesis. Certainly, exploring the dynamics of microtubular (de)polymerization in our patient may provide insight into the effects of this TUBB4B variant on intracellular trafficking. Third, as stated earlier, microtubules play a multi-faceted role in the eukaryotic cell. One study (Mechaussier et al.) (still a pre-print and had not been peer-reviewed June 2023) mounts convincing evidence that TUBB4B abnormalities are involved in ciliary dyskinesia. This raises the question of which "role" of TUBB4B is implicated in our patient's symptoms. In other words, TUBB4B can be involved in both (i) microtubule-mediated intracellular transport and (ii) building centrioles and axonemes; the questions remain how we could attribute our patient's symptoms to either (i) or (ii), Significantly, in that paper (Mechaussier et al.), two patients with TUBB4B variants exhibited renal dysfunction in addition to Leber congenital amaurosis with early-onset deafness. As the paper is still a pre-print, the clinical and genetic specifics of these patients have yet to be disclosed. Nonetheless, we maintain that renal dysfunction should not be discounted as a potential clinical manifestation of TUBB4B tubulinopathy.

5. Conclusion

As for known variants in R391 of TUBB4B, the Q11R variant can result in early onset sensory neural hearing loss with hyperopia and microcornea. However, Q11R may also be responsible for the additional phenotypic features of our patient, i.e., renal Fanconi Syndrome and rickets. One possible explanation involves impaired function of microtubules in the localization of phosphate and other transporters to the apical membranes of proximal tubular cells due to altered microtubule stability. Future mechanistic studies could explore the effects of microtubule-active drugs on the translocation of transporters for other metabolites, and whether such effects differ in magnitude in a tissue-specific manner.

Declaration of Competing Interest

None.

Data availability

Data will be made available on request.

Acknowledgment

The authors would like to thank the patient and her family in participating to this work. This work is primarily supported by the Intramural Research Programs of National Human Genome Research Institute and National Institute of Child Health and Disease from the National Institutions of Health. We also would like to thank Dr. Thomas Markello for his invaluable assistance in analyzing the genetic results from this patient.

References

[1] H.V. Goodson, E.M. Jonasson, Microtubules and microtubule-associated proteins, Cold Spring Harb Perspect Biol vol. 10 (6) (2018).
[2] α-Tubulin acetylation on lysine 40 controls cardiac glucose uptake.
[3] A. Maasz, et al., TUBB4B gene mutation in Leber phenotype of congenital amaurosis syndrome associated with early-onset deafness, Eur J Med Genet 65 (4) (2022), 104471.
[4] G.C. Rogers, S.L. Rogers, D.J. Sharp, Spindle microtubules in flux, J. Cell Sci. 118 (Pt 6) (2005) 1105–1116.
[5] R. Luscan, et al., Mutations in TUBB4B cause a distinctive sensorineural disease, Am. J. Hum. Genet. 101 (6) (2017) 1006–1012.
[6] N. Pode-Shakked, et al., Evidence of in vitro preservation of human Nephrogenesis at the single-cell level, Stem Cell Rep. 9 (1) (2017) 279–291.
[7] W. Gahl, T.C. Markello, C. Toro, K.F. Fajardo, M. Sincan, F. Gill, H. Carlson-Donohoe, A. Gropman, T.M. Pierson, G. Golas, L. Wolfe, C. Groden, R. Godfrey, M. Nehrebecky, C. Wahl, D.M. Landis, S. Yang, A. Madeo, J.C. Mullikin, D. Adams, The National Institutes of Health undiagnosed diseases program: insights into rare diseases, Genet. Med. 14 (1) (2012) 51–59.
[8] W.A. Gahl, J.J. Mulvihill, C. Toro, T.C. Markello, A.L. Wise, R.B. Ramoni, D. R. Adams, C. Tifft, The NIH undiagnosed diseases program and network: applications to modern medicine, Mol. Genet. Metab. 117 (4) (2016) 393–400.
[9] W.A.T. Gahl, C. J, The NIH undiagnosed diseases program: lessons learned, Jama 305 (18) (2011) 1904–1905.
[10] H. Chao, M. Davids, E. Burke, J. Pappas, J. Rosenfeld, A. McCarty, T. Davis, L. Wolfe, C. Toro, C. Tifft, F. Xia, N. Stong, T. Johnson, C. Warr, S. Yamamoto, D. Adams, T. Markello, W. Gahl, H. Bellen, M. Wangler, M. Malicdan, A syndromic neurodevelopmental disorder caused by De novo variants in EBF3, Am. J. Hum. Genet. 100 (1) (2017) 128–137.
[11] M. Davids, M. Kane, M. He, L. Wolfe, X. Li, M. Raihan, K. Chao, W. Bone, C. Boerkoel, W. Gahl, C. Toro, Disruption of Golgi morphology and altered protein glycosylation in PLA2G6-associated neurodegeneration, J. Med. Genet. 53 (3) (2016) 180–189.
[12] T. Markello, T. Han, H. Carlson-Donohoe, C. Ahaghotu, U. Harper, M. Jones, S. Chandrasekharappa, Y. Anikster, D. Adams, W. Gahl, C. Boerkoel, Recombination mapping using Boolean logic and high-density SNP genotyping for exome sequence filtering, Mol. Genet. Metab. 105 (3) (2012) 382–389.
[13] S. Bhagwat, D. Chandrasekhar, T. Matthew, K. Acharya, R. Gajbhiye, V. Kulkarni, S. Sonawane, M. Ghosalkar, P. Parte, Acetylated a-tubulin is reduced in individuals with poor sperm motility, Fertil. Steril. 101 (1) (2014) 95–104.
[14] C.M. Logan, C.J. Bowen, A.S. Menko, Functional role for stable microtubules in lens fiber cell elongation, Exp. Cell Res. 362 (2) (2018) 477–488.
[15] V. Pavone, et al., Hypophosphatemic rickets: etiology, clinical features and treatment, Eur. J. Orthop. Surg. Traumatol. 25 (2) (2015) 221–226.
[16] E. Renguet, α-Tubulin acetylation on lysine 40 controls cardiac glucose uptake, Am. J. Phys. 322 (6) (2022) H1032–H1043.
[17] C. Srimaroeng, J.P. Cecile, R. Walden, J.B. Pritchard, Regulation of renal organic anion transporter 3 (SLC22A8) expression and function by the integrity of lipid raft domains and their associated cytoskeleton, Cell. Physiol. Biochem. 31 (2013) 565–578.